Journal of Pharmacy & Allied Medicine

JPAM, 4(1), 01-12, 2026
https://doi.org/10.58985/jpam.2026.v04i01.39
ISSN (Print): 3005-2726

Research Article

Obtaining biologically active composites of arabinogalactan with betulin and L-histidine and studies of their physicochemical properties

Tatyana Petrovna Shakhtshneider[1*], Evgeniya Sergeevna Skurydina[2], Svetlana Anatolevna Myz[1], Svetlana Alekseevna Kuznetsova[2] and Igor Olegovich Lomovskiy[1]

1. Institute of Solid State Chemistry and Mechanochemistry SB RAS, Novosibirsk, Russia.
2. Institute of Chemistry and Chemical Technology SB RAS Federal Research Center "Krasnoyarsk Scientific Center of the SB RAS",Krasnoyarsk, Russia.

Article Information
Received: 17 December 2025
Revised: 14 January 2026
Accepted: 14 January 2026
Published: 29 January 2026

Academic Editor
Prof. Dr. Christian Celia

Corresponding Author
Prof. Dr. Tatyana Petrovna Shakhtshneider
E-mail: shah@solid.nsc.ru, shah_54@mail.ru
Tell: +79139534728

Keywords
Arabinogalactan, betulin, L-histidine, ball milling, biologically active composites, amorphization, solubilization.

Abstract

Betulin, isolated from birch bark, is a valuable biologically active substance that exhibits a wide range of pharmacological activities. However, the poor water solubility of betulin limits its use in medical and pharmaceutical applications. Arabinogalactan is a biodegradable, water-soluble natural polysaccharide, that is is primarily isolated from larch wood. Mechanochemical technologies are increasingly recognized for their sustainability, environmental benefits, and efficiency in synthesizing a wide range of chemicals and materials. In this study, ball milling was used to obtain biologically active composites of betulin with arabinogalactan in binary and ternary systems using a heterocyclic α-amino acid L-histidine as a betulin co-former. The formation of mechanocomposites was confirmed by X-ray phase analysis, IR spectroscopy and thermal analysis. The intermolecular interactions of betulin with L-histidine and arabinogalactan inhibit drug crystallization, maintaining its molecular distribution in the biopolymer. Due to antioxidant properties of L-histidine, which is used to treat rheumatoid arthritis, ulcers, anemia, and other diseases, new pharmaceutical properties of the composites can be expected. When the obtained mechanocomposites were dissolved in water, a higher concentration of betulin in solution was achieved, compared to the solubility of the initial substance, due to the distribution of the drug in the polymer and stabilization of its amorphous structure.

1. Introduction

Arabinogalactan (AG) is a biodegradable, water-soluble natural polysaccharide belonging to the hemicellulose group, which is primarily isolated from larch wood (*Larix* species). Arabinogalactan exhibits low toxicity and a range of unique properties, including immunomodulatory, prebiotic, and hepatoprotective activities [1, 2]. Several studies have shown that AG can be used as a drug carrier [3–7].

Mechanochemical methods have also been employed to obtain solid dispersion systems of drugs with arabinogalactan [5–7].

Mechanochemical technologies are increasingly recognized for their sustainability, environmental benefits, and efficiency in synthesizing a wide range of chemicals and materials, including organic compounds, biomass resource processing, synthesis

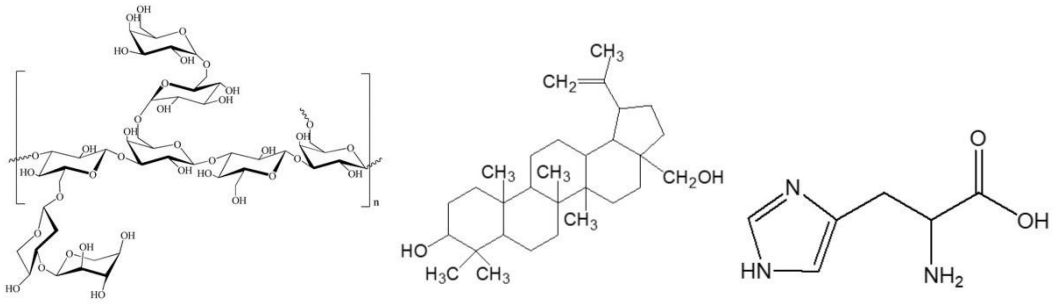

Figure 1. Molecular structures of arabinogalactan (a), betulin (b), and L-histidine (c).

and improvement of pharmaceuticals [8–10]. For improving the dissolution of pharmacologically active substances, along with obtaining amorphous drug–polymer dispersions, a promising approach has recently been proposed to obtain co-amorphous systems using mechanochemical methods among other techniques [11]. In co-amorphous systems, a drug is stabilized in the amorphous form using low molecular weight compounds known as co-formers. The low molecular weight co-formers interact with the drug on the molecular level (e.g., salt formation, hydrogen bonding, π-π interactions) or by molecular mixing, efficiently preventing drug crystallization. Amino acids, organic acids, sugars, etc. can act as co-formers [12–16]. Studies focusing on co-amorphous systems with amino acids, including L-histidine, have demonstrated that the dissolution rate of poorly water-soluble drugs can be increased, while the physical stability of formulations was maintained upon storage [15–16]. The addition of a third component, most typically a polymer, to a binary system significantly contributes to the stability of the drug in the amorphous state, particularly by increasing its glass transition temperature [11, 17]. Therefore, the dissolution of biologically active substances was improved in ternary systems, and the long-lasting formation of supersaturated solutions due to the "spring-parachute" effect was observed [18]. The third component was usually a polymeric compound such as polyvinylpyrrolidone, hydroxypropyl methylcellulose, microcrystalline cellulose, etc. [11]. To the best of our knowledge, arabinogalactan has never been used as a third component to improve drug dissolution. Meanwhile, the application of biodegradable polymers for solubilizing drugs, especially those of natural origin, is important from the perspective of green chemistry principles [19].

Betulin, isolated from birch bark, is a valuable biologically active substance exhibiting a wide range of pharmacological activities including anti-inflammatory, gastro- and hepatoprotective, antioxidant, antitumor activities [20–22]. However, the poor water solubility of betulin limits its use in medical and pharmaceutical applications. We have previously obtained binary mechanocomposites of betulin and its derivatives with water-soluble polymers, polyethylene glycol and polyvinylpyrrolidone [23]. The formation of molecular complexes of betulin diacyls with AG during mechanical activation has also been reported [6, 7]. The resulting mechanocomposites were characterized by the increased concentration of betulin diacyls in water upon dissolution.

In this study, L-histidine was selected as a co-former for betulin. L-histidine, a heterocyclic α-amino acid, is used to treat rheumatoid arthritis, ulcers and anemia. It increases gastric secretory activity and intestinal motility, improves liver function, promotes tissue growth and repair, and exhibits antioxidant properties [24, 25]. It can be expected that the use of L-histidine as a co-former will both improve the bioavailability of betulin and yield new pharmacologically important properties of preparations, possibly due to the synergistic effect.

Fig. 1 shows the molecular structures of AG, betulin, and L-histidine. The AG macromolecule (Fig. 1a) has a branched structure [1, 2, 26]: its main chain consists of galactose units linked by glycosidic bonds β-(1→3), and the side chains with β-(1→6) bonds consist of

https://doi.org/10.58985/jpam.2026.v04i01.39

galactose and arabinose units, single arabinose units, and uronic acids, mainly glucuronic acid. The functional groups in betulin (Fig. 1b) are the primary and secondary hydroxyl groups, as well as the double bond in the isopropenyl group of the five-membered ring. The hydroxyl groups of arabinogalactan can potentially form hydrogen bonds with the OH groups of betulin. When obtaining the binary and ternary systems of betulin comprising L-histidine (Fig. 1c), the OH and NH groups of the amino acid can participate in the formation of hydrogen bonds with the OH groups of the components.

The objective of the present work was to obtain the binary mechanocomposites of betulin with arabinogalactan, as well as with L-histidine as a co-former, and the ternary composites of betulin with arabinogalactan and L-histidine, and to study the effect of arabinogalactan and L-histidine on stabilization of the amorphous state of betulin and its solubilization.

2. Materials and methods

2.1. Materials

Larch wood (*Larix Sibirica*) arabinogalactan (Fibrolar DC, Wood Chemistry LLC, Russia) was used in this study. The molecular weight of AG assessed by gel permeation chromatography analysis was $M_w \approx 28{,}000$ g mol^{-1}. Betulin was obtained from birch bark (*Betula pendula* Roth.) using the reported procedure [20]. According to the data obtained by chromatography – mass spectrometry, the betulin content in the resulting substance was 97–98%. L-histidine (Panreac, Spain, CAS: 71-00-1) and 1,4-dioxane (analytical grade, CJSC Khimreaktivsnab, Russia) were used without preliminary purification or drying.

2.2. Preparation of mechanocomposites

In this study, a Pulverisette 7 premium line planetary micromill (FRITSCH GmbH, Germany) was used for ball milling of drugs, as it allows one to ground and mix the powders, and carry out the mechanochemical synthesis of novel compounds using small amounts of substances.

The betulin–L-histidine mechanocomposites were prepared by treating betulin–L-histidine powder mixtures (1:1 and 1:2 molar ratios) in a Pulverisette 7 premium line planetary micromill in 80 mL zirconium dioxide grinding jars with ZrO_2 balls (10 mm in diameter). The rotational speed of the grinding jars was 800 rpm. Taking into account the fact that liquid-assisted grinding processes are superior to neat grinding because solvent facilitates molecular diffusion and allows the interaction between the components to proceed through the liquid phase [27, 28], 0.1 mL of dioxane was added to the system after the first cycle of mechanical milling. The resulting paste was then processed in the mill for another 10 or 25 min, divided into 5-min cycles.

To obtain betulin–AG mechanocomposites, the powders of these substances were ball milled at a 1:9 mass ratio in the Pulverisette 7 premium line planetary micromill under the aforementioned conditions. Treatment duration was 15 or 30 min, divided into 5-min cycles with breaks for jar cooling.

The ball-milled ternary betulin–L-histidine–AG system was obtained by mechanically treating the powder mixtures at 3:1:28 and 1.5:1:14 mass ratios (corresponding to betulin–L-histidine 1:1 and 1:2 molar ratios, respectively, and betulin–AG 1:9 mass ratio) in a Pulverisette 7 premium line micromill. Six mechanical activation cycles were carried out, for five minutes each. To determine the effect of the order of component addition to the mixture during mechanical treatment and the solvent addition to the ternary system, two methods for obtaining mechanocomposites were tested: (1) the betulin–L-histidine mixture was milled for 5 min, and 0.1 mL of dioxane was then added to the mixture. The resulting paste was treated for 10 min. Next, AG was added to the mixture, and grinding continued for another 15 min; (2) the betulin–AG mixture was mechanically treated for 15 min. L-histidine was then added to the mixture and treated for 15 min.

2.3. Characterization of the obtained mechanocomposites

Powder X-ray diffraction (PXRD) analysis was performed using a DRON-3 diffractometer (Bourevestnik JSC, Russia), with CuK_α radiation. *Fourier transform infrared (FTIR) spectra were recorded* using an IRTracer-100 IR-Fourier spectrometer (Shimadzu, Japan) in the wavelength range of 4000–400 cm^{-1}. Samples for analysis were prepared as KBr pellets (3 mg sample/1000 mg KBr). Thermogravimetry (TG) and differential scanning

https://doi.org/10.58985/jpam.2026.v04i01.39

calorimetry (DSC) were performed using a STA 449 F1 and STA 449 C (Netzsch, Germany) simultaneous thermal analysis systems. The measurements were performed in an argon flow (99.990%) at a volumetric flow rate of 50 mL min^{-1}. The heating rate was 10°C min^{-1}. To measure the glass transition temperature T_g, the AG sample was heated to 200°C to remove water, then cooled to room temperature, and heated again. The T_g was measured as the onset of the peak.

The solubility of the mechanocomposites was studied using a Varian 705 DS Dissolution Apparatus (USA) according to the earlier method [28]. Considering that the betulin content in different composites was different, the mass of the samples required for dissolution was calculated to ensure that their betulin content was the same. The betulin concentration in water was determined by high-performance liquid chromatography (HPLC) on a Milichrom A-02 microcolumn chromatography system (EcoNova, Russia) with an UV detector. The chromatographic conditions were as follows: N2301 column 2.0×75 mm, sorbent ProntoSIL 120-5C18 AQ, particle size 5.0 μm, mobile phase H_2O (A) –CH_3CN (B), gradient mode 80-100-100% B. The aliquot volume was 2 μL. The eluent flow rate was 100 μL/min, and T=35 °C. The detection was performed at a wavelength of 200 nm.

3. Results and discussion

3.1. Synthesis and characterization of betulin–L-histidine composites

The XRD pattern of betulin treated in a mill (Fig. 2) was characterized by the broadening of the diffraction peaks and changes in their intensity, indicating the structural disordering and partial amorphization of betulin. The partial amorphization of betulin was also observed previously during the mechanical treatment of betulin in other milling devices [23].

After milling the betulin–L-histidine mixture, the intensity of the reflections decreased and some reflections in the diffraction pattern almost disappeared (Fig. 3). Furthermore, a comparison of the results of the mechanical treatment of betulin–L-histidine mixture (Fig. 3) and betulin alone (Fig. 2) clearly demonstrated that the intensity of reflections of betulin ball-milled individually was higher, regardless of milling duration. It can be assumed that the presence of L-histidine makes the amorphous state of betulin more stable under mechanical treatment compared to the case when betulin was ball-milled individually. Hence, although L-histidine used as a co-former did not cause formation of a completely amorphous composite, it still had a significant effect on the disordering of the betulin structure under mechanical treatment, and its application can be useful for betulin solubilization.

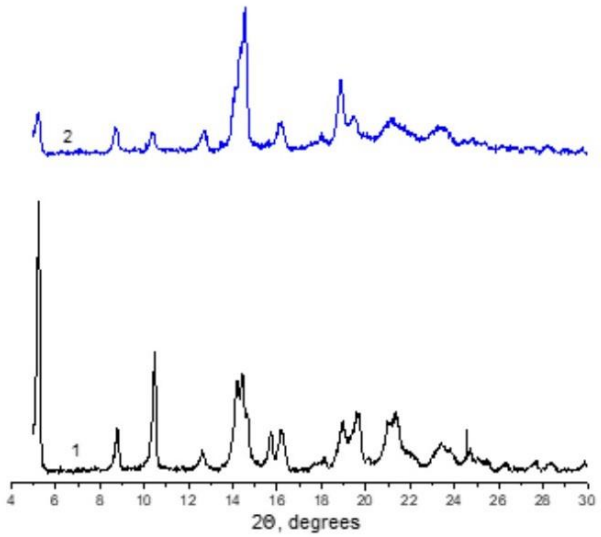

Figure 2. PXRD patterns of initial betulin (1) and betulin ball-milled for 30 min (2).

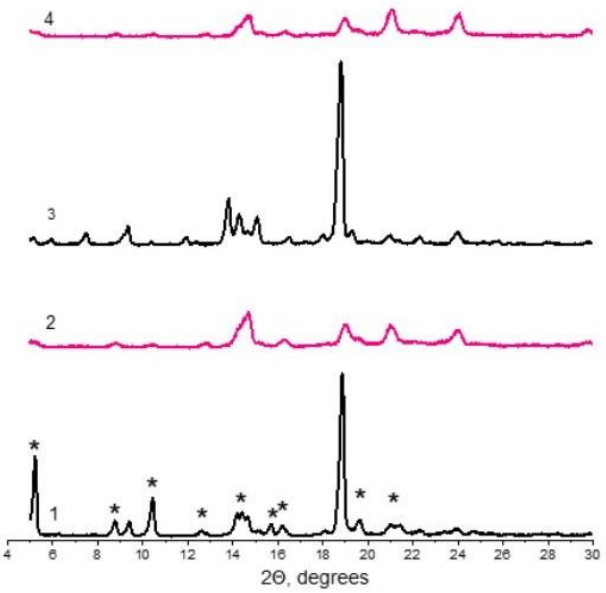

Figure 3. PXRD patterns of the 1:1 (mol) betulin–L-histidine mixture: starting (1) and after 30-min ball milling (2); 1:2 (mol) betulin–L-histidine mixture: starting (3) and after 30-min ball milling (4). L-histidine reflections are marked with an asterisk.

https://doi.org/10.58985/jpam.2026.v04i01.39

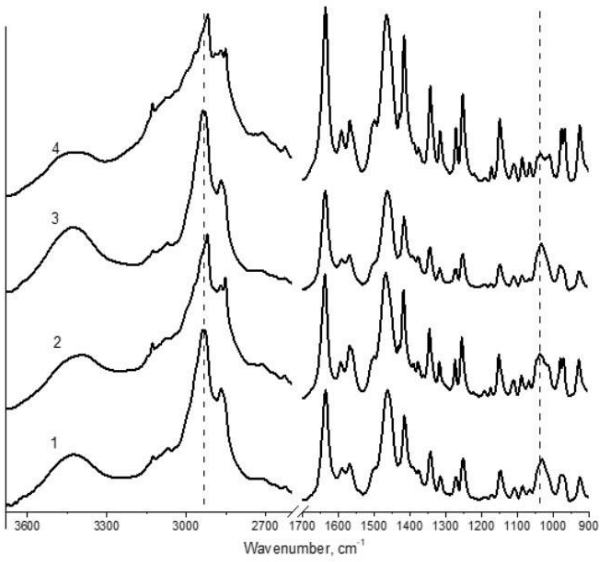

Figure 4. FTIR spectra of betulin–L-histidine mixtures with molar ratios of components 1:1 (1, 2) and 1:2 (3, 4) ball-milled separately (1, 3) and together (2, 4).

The FTIR spectra of mechanically treated 1:1 and 1:2 (mol) betulin–L-histidine mixtures, compared with the physical mixtures of the components ball-milled separately at the same ratios, are shown in Fig. 4.

In the FTIR spectra of ball-milled betulin–L-histidine mixtures, blurring of the absorption bands was observed within the region of stretching vibrations of hydroxyl groups (3300–3600 cm^{-1}), compared to the corresponding absorption bands of the physical mixtures of the components ball-milled separately. In addition, in the FTIR spectra of the ball-milled betulin–L-histidine mixtures, a change in the contour and a shift in the absorption band maximum toward the low-frequency region (from 2920 to 2900 cm^{-1}) was observed within the region of ν(=C-H) vibrations of betulin. Furthermore, the contours of the absorption band corresponding to the stretching vibrations of the N-H groups of L-histidine (2800–3200 cm^{-1}) and the band at 1020 cm^{-1} corresponding to the ν(C-O) vibration in the betulin molecule changed. The changes in the spectrum of the betulin–L-histidine mixture with a 1:2 (mol) ratio were more pronounced than those with a 1:1 (mol) ratio, especially within the regions of 2800–2900 cm^{-1} and 1000–1050 cm^{-1}. It can be assumed that during mechanical treatment, the components interact with the formation of hydrogen bonds between the OH groups of betulin and the amino groups of L-histidine. In the case of 1:2 (mol) betulin–L-histidine mixture, the amount of betulin bound to L-histidine is greater than that for the 1:1 mixture.

In the DSC curve of the initial betulin (Fig. 5a), as shown earlier [29, 30], the broad endothermic peak at low temperatures can be explained by the removal of H_2O molecules. The peak at T_{max} = 255°C corresponds to the melting of orthorhombic betulin, which was followed by degradation of the substance. The thermal effect before melting can be attributed to polymorphic transformation of betulin. Previously [30], in the X-ray thermo-diffraction experiment, we observed two polymorphic transitions of betulin: in the temperature range of 110–120°C, there was a transition to an intermediate crystalline form (betulin II), which transformed into the orthorhombic form of betulin (betulin I) before melting. On the DSC curves, the transition temperatures of endothermic effects were not constant and depended on the heating conditions (determined by kinetic factors) [30].

In the DSC curve of the ball-milled betulin–L-histidine mixture (Fig. 5c), the crystallization of betulin was observed (T_{peak} = 110°C), followed by polymorphic transitions ($T_{peak\ 1}$ = 160°C; $T_{peak\ 2}$ = 210°C) and betulin melting (T_{peak} = 252°C). This indicated that betulin and L-histidine were bound by weak hydrogen bonds to form molecular complexes that dissociated upon heating.

3.2. Synthesis and characterization of the composites of arabinogalactan with betulin and L-histidine

The betulin–AG and L-histidine–AG mixtures were ball milled before preparing the ternary betulin–L-histidine–AG composite.

The initial arabinogalactan was an X-ray amorphous substance (Fig. 6, curve 1). The X-ray diffraction pattern of arabinogalactan contains a halo in the 2θ range from 15° to 25°.

The PXRD patterns of the betulin–AG mixtures obtained by mechanical milling for 15 and 30 min were virtually identical (Fig. 6). The intensity of the betulin reflections decreased after 15 min treatment, and most of the reflections disappeared, which was apparently caused by the distribution of betulin in the polymer.

https://doi.org/10.58985/jpam.2026.v04i01.39

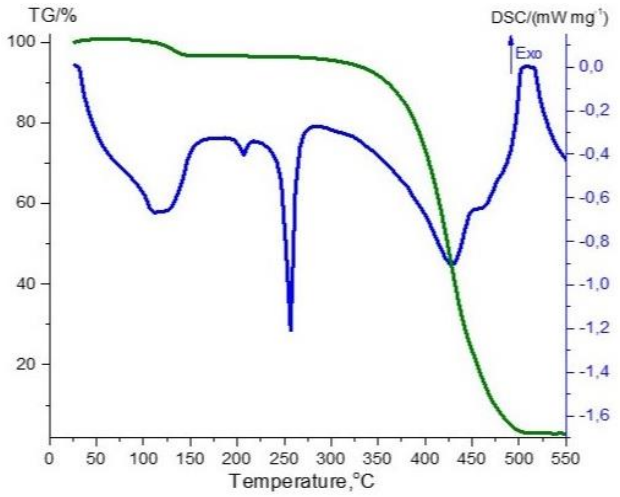

a

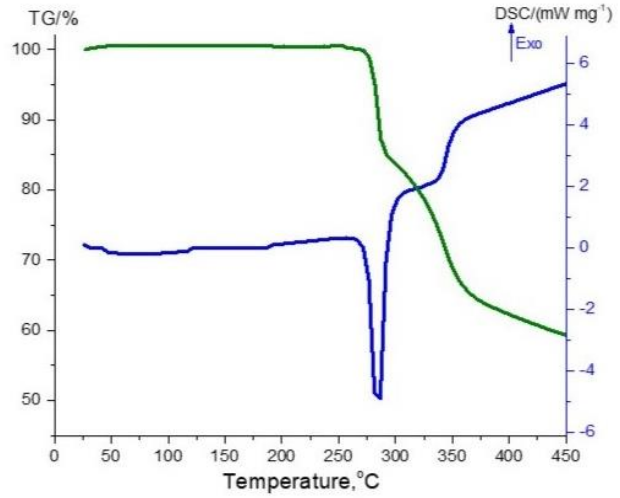

b

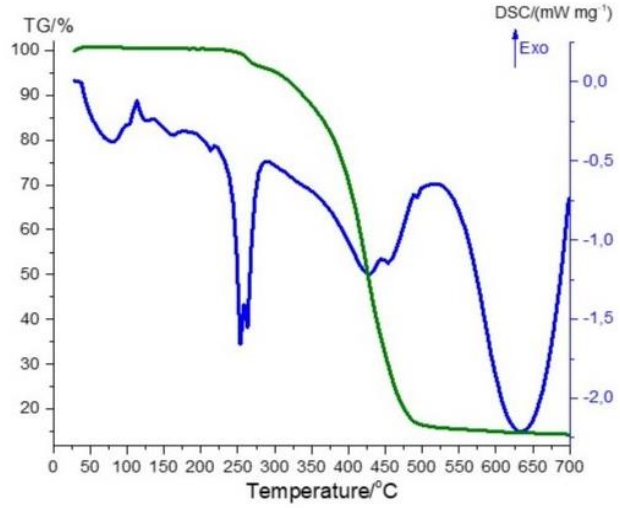

c

Figure 5. TG (green) and DSC (blue) curves of initial betulin (a) and L-histidine (b), and the ball-milled 1:2 (mol) betulin–L-histidine mixture (c) recorded during heating.

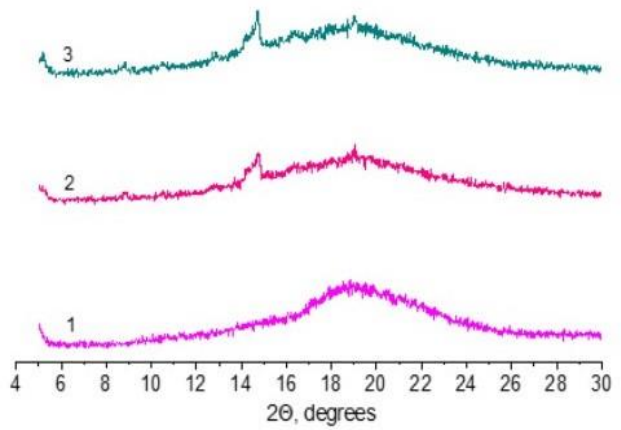

Figure. 6. PXRD patterns of initial AG (1) and 1:9 (w/w) betulin–AG mixtures ball-milled for 15 (2) and 30 min (3).

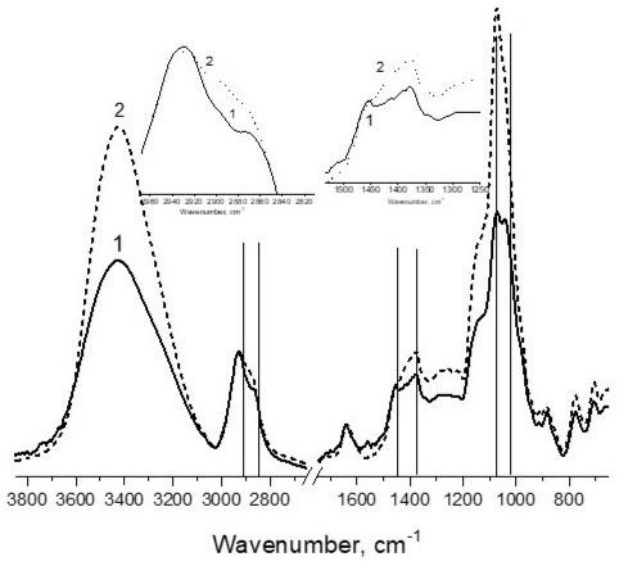

Figure 7. FTIR spectra of 1:9 (w/w) betulin–AG mixtures of the components ball-milled separately (1) and together (2). The insets show the zoomed-in images of some of the bands.

In the FTIR spectrum (Fig. 7) of the ball-milled betulin–AG mixture, compared to that of the physical mixture of the components milled separately, changes in the region of 1020–1080 cm^{-1} were observed. In this region, there are bands of stretching vibrations of C-OH in betulin and those associated with galactopyranose and arabinofuranose units in the side branches of AG [3]. As is known, during the formation of hydrogen bonds, the frequencies of the absorption bands of the groups involved in the bond can not only decrease but also increase due to the weakening of the donor bond and the strengthening of the acceptor bond. Thus, the formation of hydrogen bonds between the C-OH groups of betulin and the C-OH groups of AG can lead to a shift of the bands to higher

https://doi.org/10.58985/jpam.2026.v04i01.39

frequencies as shown in Fig. 7. The contours of the absorption bands at 1380–1450 and 2850–2920 cm^{-1} related to the vibrations of δ(CH3), ν(=C-H) and ν(C-H) also changed. The observed changes can be associated with the deformation of betulin molecules during their incorporation into the biopolymer structure or the formation of other intermolecular bonds.

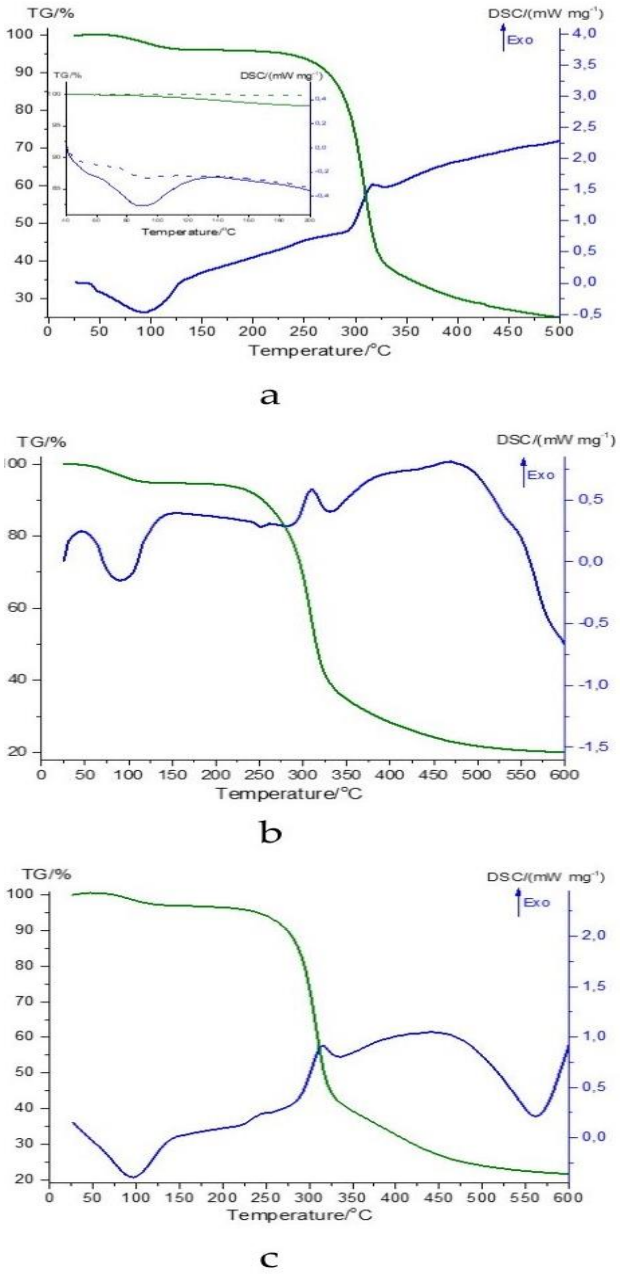

Figure 8. TG (green) and DSC (blue) curves of AG (a), the 1:9 (w/w) betulin–AG physical mixture (b), and ball-milled 1:9 (w/w) betulin–AG mixture (c) recorded upon heating. The inset in Fig. 8a shows a part of the DSC curve within the glass transition region for the first (solid line) and second (dotted line) heating.

The heating TG and DSC curves of the initial AG and ball-milled betulin–AG mixture are shown in Fig. 8. For the initial AG (Fig. 8a), adsorbed moisture was lost within a temperature interval from 80 to 150°C, followed by decomposition starting at 210°C, corresponding to the exothermic peak on the DSC curve.

It can be assumed that the endothermic effect of water removal masked the glass transition of arabinogalactan. Indeed, the DSC curve of the second heating of the AG sample (Fig. 8a) revealed a C_p jump corresponding to the glass transition, T_g, measured as 64°C.

The thermograms of the milled betulin–AG mixture (Fig. 8c) were very similar to those of AG. In contrast to the DSC curve of the betulin–AG physical mixture, neither crystallization nor melting of betulin was observed in the DSC curve of the ball-milled betulin–AG mixture, suggesting the stability of the amorphous state of betulin in its composite with AG.

The PXRD patterns of the mixtures of L-histidine with AG, ball-milled separately and together, are shown in Fig. 9. In the case of mechanical co-treatment, L-histidine was fully distributed within the polymer, resulting in an amorphous composite.

Thus, the study of binary systems showed that low molecular weight drugs were incorporated into the biopolymer to form dispersed X-ray amorphous composites.

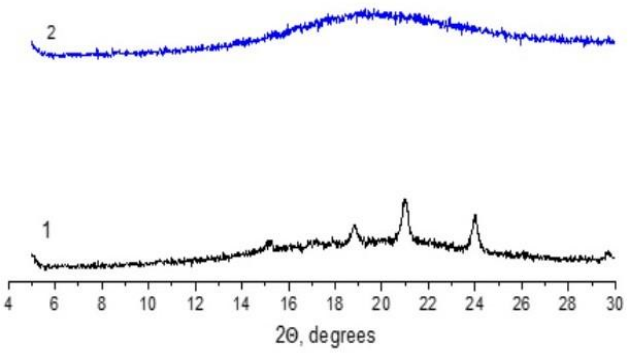

Figure 9. PXRD patterns of the 1:9 (w/w) L-histidine–AG mixtures of the components ball-milled separately (1) and together (2).

3.3. Synthesis and characterization of the composites in the ternary betulin–L-histidine–arabinogalactan system

Fig. 10 shows that the ball milling of the betulin–L-

https://doi.org/10.58985/jpam.2026.v04i01.39

histidine–arabinogalactan mixture yielded an amorphous product. The results were identical for both betulin–L-histidine–AG mixtures studied, 3:1:28 and 1.5:1:14 (w/w/w) Moreover, the sequence in which the substances were added during mechanical treatment, and the use of small amounts of dioxane, did not affect the amorphous structure of the product.

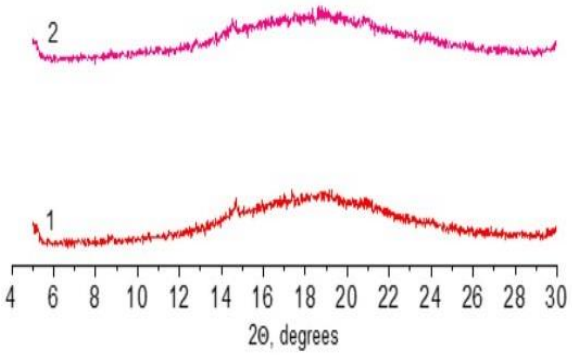

Figure 10. PXRD patterns of the 3:1:28 (w/w/w) betulin–L-histidine–AG mixture ball-milled using methods 1 (1) and 2 (2).

Considering that the reflections of betulin in the diffraction patterns of the ternary betulin–L-histidine–AG system have a much lower intensity than those of the binary betulin–AG system (Fig. 6). It can be assumed that L-histidine has an additional effect on betulin amorphization, apparently due to the interaction between these components, and both components are incorporated into the biopolymer structure. Thus, a composite was formed apparently due to the distribution of betulin and L-histidine in the polymer.

The TG and DSC curves for the ball-milled betulin–L-histidine–AG mixture are shown in Fig. 11. The endo- and exothermic effects on the DSC curve are related to water removal (50–150°C) and degradation of arabinogalactan (from 220°C), L-histidine (from 260°C), and betulin (from 320°C). Neither crystallization nor melting events occurred for betulin and L-histidine during the heating of the ternary mechanocomposite, suggesting a high physical stability of the composite.

The addition of a polymer to a binary system improves the physicochemical properties of biologically active substances and significantly contributes to the stability of drugs in the amorphous

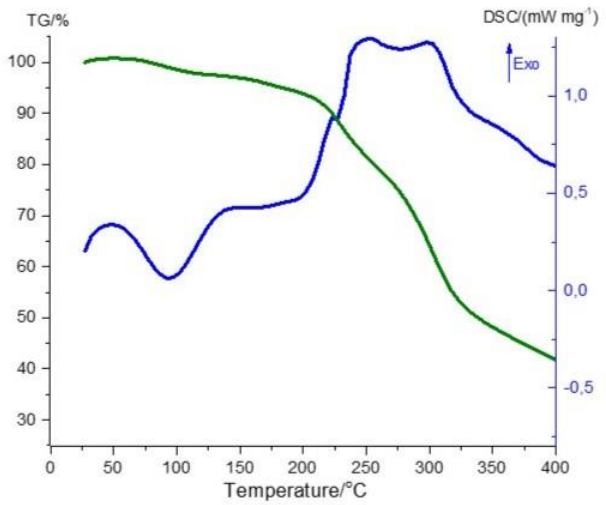

Figure 11. TG (green) and DSC (blue) curves of the ball-milled 1.5:1:14 (w/w/w) betulin–L-histidine–AG mixture recorded during heating.

state [11]. The stabilization of amorphous systems can be achieved via various mechanisms, such as the presence of intermolecular interactions, mixing at the molecular level, mutual solubility of components, and the antiplasticizing effect of the polymer [32, 33].

Arabinogalactan is expected to have an antiplasticizing effect, inhibiting drug crystallization. According to the literature, the glass transition temperature, (T_g) of arabinogalactan was 82°C [3] or 212°C [34]. The different glass transition temperature values can be attributed to the plasticizing effect of water and the differences in the molecular weights of the polymers under study. In this study, we obtained T_g = 64°C for the glass transition of arabinogalactan recorded for the dried sample. Moreover, it has been shown that mechanochemical treatment in a planetary mill AGO-2 (Russia) resulted in AG chains breaking [5]. It has also been confirmed in our work that after mechanical processing of AG in a planetary SPEX 8000 mixer mill (CertiPrep Inc., USA), its molecular weight decreases to M_w = 25,300, M_n = 18,200 g·mol^{-1} (the data will be published elsewhere). The same situation was expected to occur in our case, leading to a decline in T_g. Strictly speaking, the T_g value is not sufficiently high to raise the T_g of the mixture and decrease the mobility of the drug molecules, reducing the tendency to crystallize. Simultaneously, the intermolecular interaction of AG with betulin, which is also dependent on the suitable molecular length and optimal orientation of the

https://doi.org/10.58985/jpam.2026.v04i01.39

proton-donating and receiving groups, promotes a decrease in the mobility of the drug molecules and inhibits drug crystallization, thus maintaining its molecular distribution in the polymer.

3.4 Study of dissolution of the obtained mechanocomposites

Fig. 12 shows the dissolution profiles of the obtained binary (betulin–AG and betulin–L-histidine) and ternary, betulin–L-histidine–AG, mechanocomposites.

According to Amiri et al. [22], we measured the solubility of betulin in water, which was $1.9 \cdot 10^{-3}$ mg/mL. Upon dissolution of the betulin–AG composite in water, the initial concentration of betulin in the solution was ~ $5 \cdot 10^{-3}$ mg/mL (Fig 12a, curve 1). The formation of a supersaturated solution occurs, apparently due to the high rate of betulin release into the solution as a result of the increased dissolution area of betulin distributed in the polymer. Thus, at the initial moment, the betulin concentration in water increases by a factor of up to 2.6, compared to the solubility of the original substance. The concentration of betulin in the solution then decreased because of betulin crystallization from the supersaturated solution.

A solution with a betulin concentration of $3.5 \cdot 10^{-3}$ mg/mL was obtained upon dissolution of the betulin–L-histidine mechanocomposite (Fig. 12a, curve 2), which was retained in the solution for at least 120 min. This phenomenon can be attributed to the presence of betulin–L-histidine associates bound by hydrogen bonds in the solution. It can be assumed that betulin was released into the solution as molecular complexes with L-histidine formed during mechanical milling.

The dissolution profiles of the ternary mixtures (Fig. 12b) demonstrate that the highest concentration in the solution is observed for the betulin–L-histidine–AG composite (1.5:1:14, w/w/w) which contains the components at the following ratios: betulin–L-histidine 1:2 (mol); betulin–AG 1:9 (w/w). It can be assumed that, as in the binary system, the increased concentration was attributed to the presence of betulin–L-histidine associates in the composite and solution. In the case of the 1:2 (mol) ratio of betulin–L-histidine, more betulin molecules were associated with L-histidine, ensuring an increased concentration in the solution. On the other hand, betulin concentration in the solution, decreased rapidly,

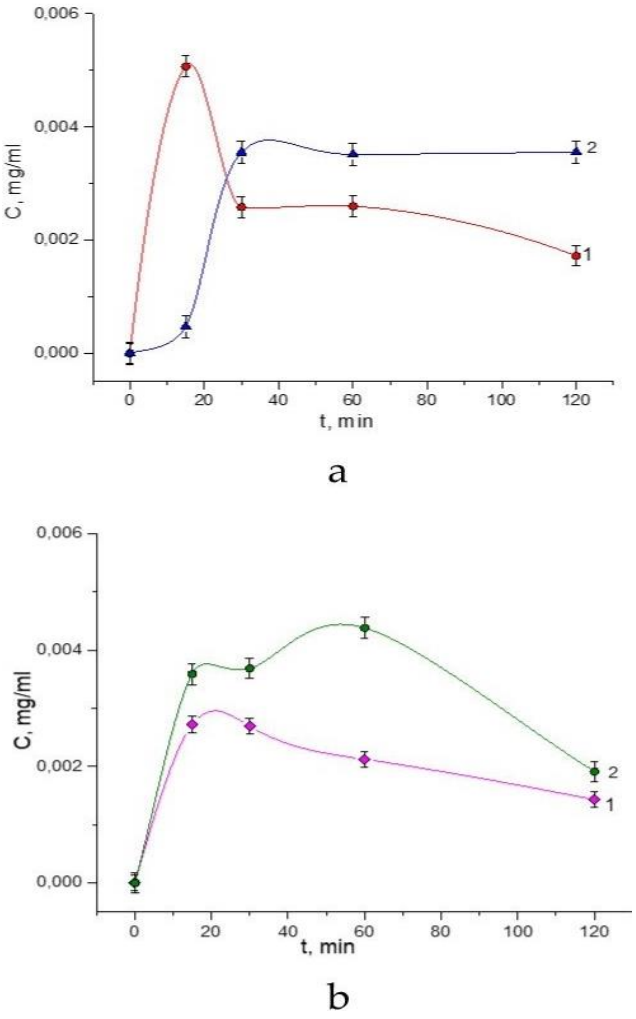

Figure 12. The profiles of betulin release from a) the binary 1:9 (w/w) betulin–arabinogalactan (1) and 1:1 (mol) betulin–L-histidine (2) mechanocomposites; b) the ternary 3:1:28 (w/w/w) (1) and 1.5:1:14 (w/w/w) (2) betulin–L-histidine–arabinogalactan mechanocomposites.

indicating that the complexes were less stable in this case than those in the binary system, as they, were associated with AG in the ball-milled ternary system. Hence, it can be assumed that the role of a co-former consists of the formation of molecular complexes with the drug, improving its dissolution.

In the literature focusing on the pharmacokinetics of betulin [35, 36], the time to reach the maximum plasma concentration in rats and dogs, (T_{max}), was estimated to range from 4 to 8 h. It is clear that direct comparison of data from *in vitro* and *in vivo* studies is impossible. To assess the solubility of a drug *in vitro*, it must be present in simulated gastric and intestinal juices for 15-30 minutes to several hours. Thus, it is necessary to ensure that the concentration of the drug

https://doi.org/10.58985/jpam.2026.v04i01.39

in the solution remains high for as long as possible.

The presented data show that for the binary mechanocomposite with arabinogalactan, the time to reach the maximum betulin concentration in the solution was ~ 10 min, with an abrupt drop during 30 min. When used in *in vivo* tests, this sample is unlikely to differ significantly from the original betulin. The binary mechanocomposite of betulin with L-histidine is the only one that provides a concentration higher than the equilibrium one for a long time, thus being the most promising candidate for further biological testing. Both ternary mechanocomposite samples have slow kinetics of concentration reaching the equilibrium concentration, the equilibrium return time is estimated to be 120 min. Whether this time is sufficient for the manifestation of significant biological effects is a question requiring additional experiments that lie beyond the scope of this study. The ternary mechanocomposite samples exhibited increased recrystallization resistance, which is important for producing final dosage forms and storage. Therefore, it will be possible to make an unambiguous choice between the more soluble but less stable binary betulin–L-histidine mixture and the less soluble but more stable ternary betulin–L-histidine–arabinogalactan mixtures with further development of the presented work.

4. Conclusions

It has been found that during mechanical treatment of the 1:9 (w/w) betulin–arabinogalactan mixture in the Pulverisette 7 premium line planetary micromill, betulin was distributed in the biopolymer, forming an X-ray amorphous product. Mechanical treatment of the mixture increased the rate of betulin dissolution in water, increasing the betulin concentration in water at the initial moment of time by a factor up to 2.6, compared to the solubility of the original substance. Nevertheless, the concentration in water declined rapidly.

Ball-milling of the betulin–L-histidine mixture with the addition of dioxane, resulted in an interaction between the triterpene alcohol and the amino acid, resulting in a higher degree of betulin amorphization, compared to betulin milled alone. Thus, L-histidine used as a co-former made the amorphous state of betulin more stable under mechanical treatment. During dissolution, the betulin–L-histidine composite provides a betulin concentration above the equilibrium level for a long time, making it the most promising candidate for further biological testing.

Under ball milling of the ternary mixture, arabinogalactan, betulin and L-histidine molecules were incorporated into the biopolymer structure to form complexes with each other and arabinogalactan. The intermolecular interaction between AG and betulin reduces the mobility of the drug molecules and inhibits drug crystallization, maintaining their molecular distribution in the polymer. The ternary betulin–L-histidine–arabinogalactan system was characterized by increased physical stability. Upon dissolution of the ternary composites, their concentration decreased to equilibrium rather slowly, additional experiments, including *in vivo* tests, are needed to assess their prospects. However, the application of ternary systems obtained by mechanical milling allows for the stabilization of betulin in an amorphous state due to the formation of stable amorphous solid dispersions that prevent crystallization and improve the dissolution rate of the insoluble substance.

Disclaimer (artificial intelligence)

Author(s) hereby state that no generative AI tools such as Large Language Models (ChatGPT, Copilot, etc.) and text-to-image generators were utilized in the preparation or editing of this manuscript.

Authors' contributions

Conceptualization, T.P.S.; data curation, E.S.S., S.A.M.; formal analysis, T.P.S., S.A.K., I.O.L.; funding acquisition: S.A.K., I.O.L.; investigation, E.S.S., S.A.M.; methodology, T.P.S., S.A.M., I.O.L.; project administration, I.O.L.; resources, S.A.K., I.O.L.; software, E.S.S., S.A.M.; validation, T.P.S., S.A.M., I.O.L.; supervision, T.P.S., S.A.M., O.L.; visualization S.A.M.; writing– original draft, T.P.S.; writing – review & editing, S.A.K., I.O.L.

Acknowledgements

The equipment of the Krasnoyarsk Regional Center for Collective Use of FRC KSC SB RAS was used in this work. The authors are grateful to G.N. Bondarenko for providing the PXRD data and S.N.

https://doi.org/10.58985/jpam.2026.v04i01.39

Vereshchagin for providing the differential scanning calorimetry results.

Funding

This research was funded by budget projects No. 124060500047-1 for the ISSCM SB RAS and No. FWES-2026-0010 for the ICCT SB RAS.

Availability of data and materials

All relevant data are within the paper. Additional data will be made available on request according to the journal policy.

Conflicts of interest

The authors declare no conflict of interest. All authors confirm that they voluntarily participated in the research.

References

1. Medvedeva, E.N.; Babkin, V.A.; Ostroukhova, L.A. Arabinogalactan of larch - Properties and prospects of use (review). Khimija Rastitel`nogo Syr`ja . 2003, 1, 27-37. (in Russ.).
2. Huang, W.; Xie, Y.; Guo, T.; Dai, W.; Nan, L.; Wang, Q.; Liu, Y.; Lan, W.; Wang, Z.; Huang, L.; Gong, G. A new perspective on structural characterisation and immunomodulatory activity of arabinogalactan in *Larix kaempferi* from Qinling Mountains. Int. J. Biol. Macromol. 2024, 265, 130859. https://doi.org/10.1016/j.ijbiomac.2024.130859
3. Thakare, K. The evaluation of larch arabinogalactan as a new carrier in the formulation of solid dispersions of poorly water-soluble drugs. Dissertations & Thesis, Ph.D, Temple Univ. p. 387, 2013.
4. Badykova, L.A.; Mudarisova, R.K.; Kolesov, S.V. Transport properties and physiological activity of arabinogalactan complexes with certain nitrogen-containing compounds. Polym. Sci. Ser. A. 2021, 63(2), 117-122. https://doi.org/10.1134/S0965545X21020012
5. Dushkin, A.V.; Meteleva, E.S.; Tolstikova, T.G.; Tolstikov, G.A.; Polyakov, N.E.; Neverova, N.A.; Medvedeva, E.N.; Babkin, V.A. Mechanochemical preparation and pharmacological activities of water-soluble intermolecular complexes of arabinogalactan with medicinal agents. Russ. Chem. Bull. 2008, 57(6), 1299-1307. https://doi.org/10.1007/s11172-008-0167-8
6. Kuznetsova, S.A.; Shakhtshneider, T.P.; Mikhailenko, M.A.; Malyar, Y.N.; Zamay, A.S.; Boldyrev, V.V. Preparation of mechanocomposites of betulin diacetate with arabinogalactan and study of their antitumor properties. SibFU J. Chem. 2013, 6(2), 192-202 (in Russ.).
7. Kuznetsova, S.A.; Shakhtshneider, T.P.; Mikhailenko, M.A.; Malyar, Y.N.; Kichkailo, A.S.; Drebushchak, V.A.; Kuznetsov, B.N. Preparation and antitumor activity of betulin dipropionate and its composites. Bioint. Res. Appl. Chem. 2022, 12(5), 6873-6894. https://doi.org/10.33263/BRIAC125.68736894
8. Mateti, S.; Mathesh, M.; Liu, Z.; Tao T.; Ramireddy, T.; Glushenkov, A.M.; Yang, W.; Chen, Y.I. Mechanochemistry: A force in disguise and conditional effects towards chemical reactions. Chem. Commun. 2021, 57, 1080. https://doi.org/10.1039/d0cc06581a
9. Shen, F.; Xiong, X.; Fu, J.; Yang, J.; Qiu, M.; Qi, X.; Tsang, D.C.W. Recent advances in mechanochemical production of chemicals and carbon materials from sustainable biomass resources. Ren. Sust. Energ. Rev. 2020, 130, 109944. https://doi.org/10.1016/j.rser.2020.109944
10. Haneef, J.; Ali, S. Medicinal mechanochemistry: Sustainable and efficient route towards synthesis of active pharmaceutical ingredients. Sust. Chem. Pharm. 2025, 45, 102044. https://doi.org/10.1016/j.scp.2025.102044
11. Aher, A.A.; Shaikh, K.S.; Chaudhari, P.D. Stability of co-amorphous solid dispersions: Physical and chemical aspects. J. Struct. Chem. 2023, 64(4), 686-738. https://doi.org/10.26902/JSC_id109666
12. Yarlagadda, D.L.; Anand, V.S.K.; Nair, A.R.; Sree, K.N.; Dengale, S.J.; Bhat, K. Considerations for the selection of co-formers in the preparation of co-amorphous formulations. Int. J. Pharm. 2021, 602, 120649. https://doi.org/10.1016/j.ijpharm.2021.120649
13. Jangid, A.K.; Jain, P.; Medicherla, K.; Pooja, D.; Kulhari, H. Solid-state properties, solubility, stability and dissolution behavior of co-amorphous solid dispersions of baicalin. Cryst. Eng. Comm. 2020, 22(37), 6128-6136. https://doi.org/10.1039/d0ce00750a
14. Liu, J.; Grohganz, H.; Löbmann, K.; Rades, T.; Hempel, N.J. Co-amorphous drug formulations in numbers: Recent advances in co-amorphous drug formulations with focus on co-formability, molar ratio, preparation methods, physical stability, in vitro and in vivo performance, and new formulation strategies. Pharmaceutics. 2021, 13(3), 389. https://doi.org/10.3390/pharmaceutics13030389
15. Kasten, G.; Lobmann, K.; Grohganz, H.; Rades, T. Co-former selection for co-amorphous drug-amino acid formulations. Int. J. Pharm. 2019, 557, 366-373. https://doi.org/10.1016/j.ijpharm.2018.12.036
16. Kapoor, D.U.; Singh, S.; Sharma, P.; Prajapati, B.G. Amorphization of low soluble drug with amino acids to improve its therapeutic efficacy: A state-of-art-review. AAPS Pharm. Sci. Tech. 2023, 24(8), 253. https://doi.org/10.1208/s12249-023-02709-2
17. Pacult, J.; Rams-Baron, M.; Chmiel, K.; Jurkiewicz, K.;

Antosik, A.; Szafraniec, J.; Kurek, M.; Jachowicz, R.; Paluch, M. How can we improve the physical stability of co-amorphous system containing flutamide and bicalutamide? The case of ternary amorphous solid dispersions. Europ. J. Pharm. Sci. 2019, 136, 104947. https://doi.org/10.1016/j.ejps.2019.06.001

18. Bavishi, D.D.; Borkhataria, C.H. Spring and parachute: How cocrystals enhance solubility. Prog. Cryst. Growth Charact. Mater. 2016, 62, 1–8. http://dx.doi.org/10.1016/j.pcrysgrow.2016.07.001
19. Anastas, P.; Eghbali, N. Green chemistry: Principles and practice. Chem. Soc. Rev. 2010, 39, 301-312. https://doi.org/10.1039/B918763B
20. Kuznetsova, S.A.; Skvortsova, G.P.; Maliar, I.N.; Skurydina, E.S.; Veselova, O.F. Extraction of betulin from birch bark and study of its physico-chemical and pharmacological properties. Russ. J. Bioorgan. Chem. 2014, 40(7), 742-747. https://doi.org/10.1134/S1068162014070073
21. Demets, O.V.; Takibayeva, A.T.; Kassenov, R.Z.; Aliyeva, M.R. Methods of betulin extraction from birch bark. Molecules. 2022, 27(11), 3621. https://doi.org/10.3390/molecules27113621
22. Amiri, Sh.; Dastghaib, S.; Ahmadi, M.; Mehrbod, P.; Khadem, F.; Behrouj, H.; Aghanoori, M.-R.; Machaj, F.; Ghamsari, M.; Rosik, J.; Hudecki, A.; Afkhami, A.; Hashemi, M.; Los, M.J.; Mokarram, P.; Madrakian, T.; Ghavami, S. Betulin and its derivatives as novel compounds with different pharmacological effects. Biotechnol. Adv. 2020, 38, 107409. https://doi.org/10.1016/j.biotechadv.2019.06.008
23. Mikhailenko, M.A.; Shakhtshneider, T.P.; Drebushchak, V.A.; Kuznetsova, S.A.; Skvortsova, G.P.; Boldyrev, V.V. Effect of mechanical processing on the properties of betulin, betulin diacetate and their mixture with water-soluble polymers. Chem. Nat. Comp. 2011, 2, 211-214. https://doi.org/10.1007/s10600-011-9889-1
24. Holeček, M. Histidine in health and disease: metabolism, physiological importance, and use as a supplement. Nutrients. 2020, 12(3), 848. https://doi.org/10.3390/nu12030848
25. Vera-Aviles, M.; Vantana, E.; Kardinasari, E.; Koh, N.L.; Latunde-Dada, G.O. Protective role of histidine supplementation against oxidative stress damage in the management of anemia of chronic kidney disease. Pharmaceuticals. 2018, 11(4), 111. https://doi.org/10.3390/ph11040111
26. Sato, K.; Hara, K.; Yoshimi, Y.; Kitazawa, K.; Ito, H.; Tsumuraya, Y.; Kotake, T. Yariv reactivity of type II arabinogalactan from larch wood. Carbohydr. Res. 2018, 467, 8-13. https://doi.org/10.1016/j.carres.2018.07.004
27. Hasa, D.; Jones, W. Screening for new pharmaceutical solid forms using mechanochemistry: A practical guide. Adv. Drug Deliv. Rev. 2017, 117, 147-61. https://doi.org/10.1016/j.addr.2017.05.001
28. Myz, S.A.; Mikhailenko, M.A.; Mikhailovskaya, A.V.; Bulina, N.V.; Gerasimov, K.B.; Politov, A.A.; Kuznetsova, S.A.; Shakhtshneider, T.P. Cocrystals of betulin with adipic acid: preparation and thermal behavior. J. Therm. Anal. Calorim. 2022, 147, 8235–8242. https://doi.org/10.1007/s10973-021-11107-4
29. Mikhailovskaya, A.V.; Myz, S.A.; Gerasimov, K.B.; Kuznetsova, S.A.; Shakhtshneider, T.P. Synthesis of cocrystals of betulin with suberic acid and study of their properties. Khimija Rastitel`nogo Syr`ja. 2021, 4, 183-192 (in Russ.). https://doi.org/10.14258/jcprm.2021049736
30. Drebushchak, T.N.; Mikhailovskaya, A.V.; Drebushchak, V.A.; Mikhailenko, M.A.; Myz, S.A.; Shakhtshneider, T.P.; Kuznetsova, S.A. Crystalline forms of betulin: Polymorphism or pseudopolymorphism? J. Struct. Chem. 2020, 61(8), 1260-1266. https://doi.org/10.1134/S0022476620080119
31. Myz, S.A.; Politov, A.A.; Shakhtshneider, T.P.; Kuznetsova, S.A. Morphology changes in betulin particles as a result of polymorphic transformations and formation of co-crystals under heating. Powders. 2023, 2(2), 432-444. https://doi.org/10.3390/powders2020026
32. Ueda, H.; Kadota, K.; Imono, M.; Ito, T.; Kunita, A.; Tozuka, Y. Co-amorphous formation induced by combination of tranilast and diphenhydramine hydrochloride. J. Pharm. Sci. 2017, 106(1), 123-128. https://doi.org/10.1016/j.xphs.2016.07.009
33. Lodagekar, A.; Chavan, R.B.; Chella, N.; Shastri, N.R. Role of valsartan as an antiplasticizer in development of therapeutically viable drug–drug coamorphous system. Cryst. Growth Des. 2018, 18(4), 1944–1950. https://doi.org/10.1021/acs.cgd.8b00081
34. Bochek, A.M.; Zabivalova, N.M.; Gofman, I.V.; Lebedeva, M.F.; Popova, E.N.; Lavrent'ev, V.K. Properties of composite films of methylcellulose with arabinogalactan. Polym. Sci. Ser. A. 2015, 57(4), 430-436. https://doi.org/10.1134/S0965545X15040021
35. Jäger, S.; Laszczyk, M.N.; Scheffler, A.A. Preliminary pharmacokinetic study of Betulin, the main pentacyclic triterpene from extract of outer bark of birch (*Betulae alba* cortex). Molecules. 2008, 13, 3224-3235. https://doi.org/10.3390/molecules13123224
36. Hu, Z.; Guo, N.; Wang, Z.; Liu, Y.; Wang, Y.; Ding, W.; Zhang, D.; Wang, Y.; Yan, X. Development and validation of an LC–ESI/MS/MS method with precolumn derivatization for the determination of betulin in rat plasma. J. Chromatogr. B Analyt. Technol. Biomed. Life Sci. 2013, 939, 38-44. https://doi.org/10.1016/j.jchromb.2013.09.005